

Phase transitions, Kauzmann curves, and inverse melting

Frank H. Stillinger^a, Pablo G. Debenedetti^{b,*}

^a*Department of Chemistry, Princeton University, Princeton, NJ 08544, USA*

^b*Department of Chemical Engineering, Princeton University, Princeton, NJ 08544, USA*

Received 5 September 2002; accepted 30 September 2002

Abstract

Walter Kauzmann's classic 1948 review of liquid supercooling and glass formation drew attention to the temperatures at which (by extrapolation) enthalpies and entropies of liquid and crystal phases would appear to become equal. In the temperature–pressure (T, p) plane, the collection of such 'Kauzmann temperatures' generate characteristic curves. The present study examines the connection of those Kauzmann loci to equilibrium inverse melting phenomena, i.e. cases where isobaric heating causes freezing of the liquid. Such cases are associated with local minima or maxima in the melting curve $p_m(T)$, and we point out the possible relevance of melting curve maxima to the thermodynamics of protein folding. Both equal-enthalpy and equal-entropy Kauzmann curves must pass through melting curve extrema. Three thermodynamic identities have been obtained to describe the vicinity of these points; they involve, respectively, the slopes of the two Kauzmann curves, and the second temperature derivative of the melting pressure. The second of these three equations is formally identical to the first Ehrenfest relation for second-order phase transitions, but carries no phase-transition implication. For purposes of specific numerical illustration, the inverse-melting behavior displayed by ³He at low temperature has been analyzed in detail.

© 2003 Elsevier Science B.V. All rights reserved.

Keywords: Kauzmann curves; Inverse melting; Kauzmann paradox

1. Introduction

It is always a pleasure to recognize and to honor the lasting scientific contributions of an esteemed colleague and friend. In the present instance, it is our good fortune to do just that for Professor Walter Kauzmann. The focus of this paper arises from the need to understand the properties of

supercooled liquids, and the glasses that they form as a result of supercooling. The historical source of the underlying ideas with which we deal below is a famous review article published by Walter Kauzmann in 1948 [1], which for good reason continues to receive frequent literature citations even today. A vast amount of research in this scientifically challenging field has occurred following appearance of that review, with a correspondingly vast array of published papers. For readers not intimately involved with supercooled liquids and glasses, it may be helpful to point out

*Corresponding author. Tel.: +1-609-258-5480; fax: +1-609-258-0211.

E-mail address: pdebene@princeton.edu (P.G. Debenedetti).

that several recent comprehensive reviews also exist, documenting the experimental and theoretical advances that have been made subsequent to 1948 [2–6].

Professor Kauzmann stressed the significance of the experimental fact that, for most liquids, upon supercooling the constant-pressure heat capacity $C_p^{(l)}(T)$ exceeds that of the thermodynamically stable crystal phase $C_p^{(c)}(T)$, with the discrepancy widening with increasing extent of supercooling. Consequently, reduction in absolute temperature T causes the metastable liquid to lose both entropy and enthalpy faster than does the stable crystal. Although a glass transition or crystal nucleation event typically would intervene to frustrate continuation of this trend to very low temperature, smooth and ‘reasonable’ extrapolation of the heat capacities indicates that the entropy of the supercooled liquid would equal that of the crystal at a positive ‘Kauzmann temperature’ T_K . Further reduction in temperature toward absolute zero, following the same extrapolation, would then produce a non-crystalline state with entropy substantially below that of the stable crystal phase, in clear violation of the third law of thermodynamics [7]. This conundrum has traditionally been called the ‘Kauzmann paradox’ [8]. An analogous enthalpy crossing would occur (at least for ‘fragile’ glass formers [3,4]) at another temperature, T_H (where $0 < T_H < T_K$), implying that the corresponding problematical non-crystalline state at $T=0$ would also be substantially lower in enthalpy than the crystal.

The notion that a supercooled liquid might run out of available molecular configurations at, or near, a Kauzmann temperature T_K , should have implications beyond thermodynamics, and so has long influenced the interpretation of flow and relaxation behavior. As an example, this has tended to provide legitimacy to the presence of a divergence temperature $T_0 > 0$ in the Vogel–Tammann–Fulcher (‘VTF’) expression for the temperature dependence of shear viscosity [9–11]. It also underlies the conceptual basis of the Adam–Gibbs theory of relaxation phenomena [12].

For obvious reasons, the majority of the experimental studies of supercooled liquids and glasses

involves ambient pressure. However, a comprehensive view of the properties of those metastable states includes the effects of varying pressure, extending even into the negative pressure (isotropic tension) regime [13,14]. In the analysis provided below, we shall be interested in examining behavior in the temperature–pressure (T,p) plane. As examples, the two temperatures just mentioned define curves $T_K(p)$ and $T_H(p)$ in that plane. These functions can be grouped with, but remain distinguished from, the familiar thermodynamic melting temperature $T_m(p)$, and the experimental convention-dependent glass-transition temperature $T_g(p)$.

Our primary objective in this paper is to elaborate upon an earlier suggestion [8], specifically that comprehensive understanding of the many-body phenomena underlying the Kauzmann paradox should include analysis of ‘inverse melting’. This unusual and counter-intuitive phenomenon involves liquids at thermodynamic equilibrium that crystallize upon isobaric addition of heat, the reverse of the usual situation. The relevance to supercooling and glass formation is that these cases permit straightforward identification of a Kauzmann $T_K(p)$ curve, at least one point of which lies on the equilibrium melting curve $T_m(p)$. This avoids the usually encountered uncertainty associated with heat capacity extrapolation below a glass transition temperature, one consequence of which has been argument in the literature [15–17] over whether or not a thermodynamic ‘ideal glass transition’ in principle should exist close to $T_K(p)$.

Section 2 identifies some known real-substance examples of the inverse melting phenomenon. Interestingly, this listing cites an example drawn from protein physical chemistry, another subject toward which Walter Kauzmann has contributed fundamental insights [18]. Section 3 analyzes thermodynamic relations for the two phases exhibiting the inverse-melting property, and deduces families of curves in the T,p plane that describe constant entropy differences (generalized Ehrenfest relations), as well as curves of constant enthalpy differences, between the two phases of interest. Section 4 is devoted to the specific case of the lighter helium isotope ^3He and its inverse melting behavior. Final remarks have been collected into a concluding Section 5, where we speculate on the

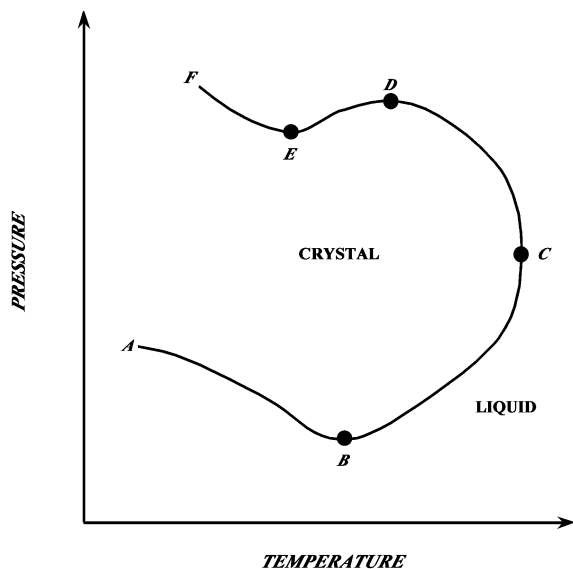


Fig. 1. Schematic melting curve in the T,p plane, to illustrate various melting circumstances, including the inverse-melting phenomenon.

possibilities of synthesizing and studying new materials for laboratory study, and of devising new models for theoretical analysis, that might display the inverse melting phenomenon.

2. Inverse-melting systems

An appropriate starting point for discussion of the inverse melting phenomenon is the Clausius–Clapeyron equation that describes the slope of the melting curve in the T,p plane [19]:

$$dp_m(T)/dT = (S^{(l)} - S^{(c)}) / (V^{(l)} - V^{(c)}) \quad (2.1)$$

Here, $p_m(T)$ is the temperature-dependent melting pressure, the function that is the inverse of $T_m(p)$. Molar entropies and volumes are denoted by $S^{(v)}$ and $V^{(v)}$, with superscripts $v=l,c$ indicating liquid and crystal phases, respectively.

By way of illustrating the relevance of thermodynamic identity [Eq. (2.1)] to the inverse melting scenario, Fig. 1 offers a schematic melting curve $ABCDEF$. This will help to classify the known examples of this phenomenon. It will be assumed that the liquid–crystal phase transition remains first

order along this entire curve, so at least one of $S^{(l)} - S^{(c)}$ and $V^{(l)} - V^{(c)}$ is non-zero at every point of the curve. It will further be assumed that only a single crystal phase is involved, at least in the region of the T,p plane depicted in Fig. 1.

The familiar ‘normal’ melting scenario involves an increase in molar volume upon melting of the crystal, which occurs as the system absorbs the latent heat of transition. Consequently, in the right member of the Clausius–Clapeyron Eq. (2.1), both the numerator $S^{(l)} - S^{(c)}$ as well as the denominator $V^{(l)} - V^{(c)}$ are positive, and so the slope of $p_m(T)$ is positive. This circumstance corresponds in Fig. 1 to the portion of the full curve that lies between points B and C .

Less common, though still familiar, is the case in which the molar volume decreases upon melting the crystal, while again heat is absorbed in the melting process. This combination changes the sign of the melting curve slope, and corresponds to the portions of the curve shown in Fig. 1 that lie between points C and D , and between E and F . Examples of real substances exhibiting this behavior (at modest pressures) are the elements silicon, gallium, antimony, and bismuth [20], and of course the familiar molecular substance water [21]. The point C in Fig. 1 locates the position at which the molar volumes of coexisting crystal and liquid are identical, which Eq. (2.1) requires to be a point of infinite slope of the melting curve $p_m(T)$.

The intervals between points A and B , and between points D and E , are ranges of inverse melting. Starting in the liquid phase just to the left of either of these intervals, isobaric heating causes crossing of the phase transition curve, i.e. causes the system to freeze into the crystalline phase. That such a counter-intuitive inverse melting might occur in the real world was apparently first suggested by Tammann a century ago [22]. Inverse melting is characterized by the entropy inequality:

$$S^{(l)} - S^{(c)} < 0 \quad (2.2)$$

The interval AB exhibits negative slope, while the interval DE exhibits positive slope, because $V^{(l)} - V^{(c)}$ is positive for the former, but negative for the latter.

The three points B , D and E are distinguished by vanishing of the melting curve slope:

$$dp_m(T)/dT=0 \quad (B,D,E) \quad (2.3)$$

These points thus are all associated with vanishing entropy change:

$$S^{(l)} - S^{(c)} = 0 \quad (B,D,E) \quad (2.4)$$

because the difference in molar volumes can never be infinite. Consequently, these are ‘Kauzmann points’ occurring as natural loci in the equilibrium phase diagram. Their existence does not hinge upon the legitimacy of long heat capacity extrapolations that are obliged to cross glass transitions. Section 3 utilizes this identification to trace out ‘Kauzmann curves’ $T_K(p)$ as they pass through these kinds of distinguished points. Notice also that B , D and E must lie on vanishing–enthalpy curves $T_H(p)$. This follows from the fact that at any point along the melting curve, the chemical potentials of the coexisting phases are equal, and hence the respective enthalpy and entropy differences satisfy $\Delta H = T\Delta S$.

With this schematic analysis as background, we can now classify examples of inverse melting that have been reported in the published literature. The best-documented examples of inverse melting are the two helium isotopes ^3He [23] and ^4He [24,25] at low temperature. Both isotopes display melting curves that qualitatively resemble the neighborhood of point B in Fig. 1, but they differ significantly from one another in quantitative detail. The ^3He example has its zero-slope minimum at approximately 0.315 K and 29.3 bar, with normal (i.e. non-superfluid) liquid in coexistence with body-centered cubic crystal. By contrast, the ^4He minimum is very shallow, occurs at approximately 0.8 K and 26.2 bar, and has superfluid liquid in coexistence with hexagonal-close-packed crystal. The ^3He case will be examined in numerical detail in Section 4.

A very different inverse-melting material has recently come to attention. This is the polymeric substance poly(4-methylpentene-1), denoted more simply as ‘P4MP1’ [26–29]. Published reports indicate that its melting curve in the T,p plane

possesses a maximum of the type depicted in Fig. 1 by point D and its neighborhood. The crystalline phase in coexistence with the liquid has been reported to be tetragonal. This melting maximum occurs at approximately 425 K and 6.5 kbar. The P4MP1 and helium isotope examples have been mentioned in a previous publication as relevant to the Kauzmann paradox issue [8].

Although smaller by many orders of magnitude than macroscopic phases, individual protein molecules in solution possess, nevertheless, a large number of internal conformational degrees of freedom. The rather sharp transition between the structurally organized and biologically relevant native form, and the large group of biologically inactive denatured forms, provides a strong analogy to the conventional melting transition. It is therefore satisfying to notice that at least one protein, ribonuclease A, displays a ‘melting’ curve in the T,p plane with a maximum of type D in Fig. 1. This maximum is located approximately at 283 K and 4.0 kbar, with the native form lying below the maximum, and the denatured form above the maximum [30]. Starting at a slightly lower temperature and pressure, an initially denatured molecule can be induced to renature at constant pressure by raising the temperature. By semantic analogy to the phrase ‘inverse melting’, this process might well be called ‘inverse denaturation’.

Liquid crystals also supply a useful analogy to inverse melting. Basing his remarks on data reported by Cladis et al. [31], Johari has pointed out that the first-order phase boundary between the smectic-A and nematic phases of 4-cyano-4'-octyloxybiphenyl also exhibits a maximum in the T,p plane (type D in Fig. 1) [32]. This maximum occurs at approximately 350 K and 2100 bar. In fact, the observed phase boundary is analogous to a larger portion of the schematic curve in Fig. 1 that includes a point of equal molar volumes for the two coexisting phases (type C in Fig. 1). Starting at the appropriate nematic state (possessing just molecular orientational order), isobaric heating can cause the material to reorder into the smectic-A phase (possessing both orientational and partial translational order).

The reader should be warned that the scientific literature also uses the phrase ‘inverse melting’ in

a circumstance that is not directly relevant to the present study. In particular, kinetically-controlled irreversible transformations of supersaturated alloy crystals to amorphous solids under heat treatment have been described this way [33].

3. Generalized Ehrenfest relations

In order to present a proper thermodynamic characterization of inverse melting phenomena, it will be useful and convenient to use leading terms of Taylor expansions for properties of interest. For the moment, let X represent any zero-slope point of the melting curve (such as B , D and E in Fig. 1). We shall suppose that thermodynamic functions are well defined for both phases in the vicinity of X . The temperature and pressure at this point will be denoted by T_X and p_X , respectively. Near point X , the molar volumes of the two phases formally have the following series expansions ($v=c,l$):

$$V^{(v)}(T,p) = V^{(v)}(X) + A^{(v)}\delta T + B^{(v)}\delta p + \dots$$

$$\delta T = T - T_X, \quad \delta p = p - p_X \quad (3.1)$$

where subsequent terms involve quadratic and higher-order combinations of the deviations δT and δp . The linear coefficients $A^{(v)}$, $B^{(v)}$ are related to the isobaric thermal expansions $\alpha^{(v)}$ and isothermal compressibilities $\kappa_T^{(v)}$ evaluated at position X :

$$A^{(v)} = \alpha^{(v)}(X)V^{(v)}(X)$$

$$B^{(v)} = -\kappa_T^{(v)}(X)V^{(v)}(X) \quad (3.2)$$

Similar expansions express the behavior of the molar phase enthalpies in the neighborhood of point X . Starting with the thermodynamic identities

$$\left(\frac{\partial H}{\partial T}\right)_p = C_p$$

$$\left(\frac{\partial H}{\partial p}\right)_T = V(1 - \alpha T) \quad (3.3)$$

the expansions for the separate phases will appear as follows:

$$H^{(v)}(T, p) = H^{(v)}(X) + C_p^{(v)}(X) \delta T + V^{(v)}(X) [1 - T_X \alpha^{(v)}(X)] \delta p + \dots \quad (3.4)$$

Recalling that the zero-slope point X has the property that molar enthalpies are exactly equal there, we deduce a linear expression for the difference in molar enthalpies of the liquid and crystal phases that is locally valid in the vicinity of point X :

$$H^{(l)}(T, p) - H^{(c)}(T, p) \cong [C_p^{(l)}(X) - C_p^{(c)}(X)] \delta T + \{V^{(l)}(X)[1 - T_X \alpha^{(l)}(X)] - V^{(c)}(X) [1 - T_X \alpha^{(c)}(X)]\} \delta p \quad (3.5)$$

For any fixed value of the enthalpy difference between the phases, δp is a linear function of δT :

$$\delta p = \eta - \left\{ \frac{C_p^{(l)} - C_p^{(c)}}{[V^{(l)}(1 - T\alpha^{(l)}) - V^{(c)}(1 - T\alpha^{(c)})]} \right\}_X \delta T,$$

$$\eta = \frac{H^{(l)} - H^{(c)}}{\{V^{(l)}[1 - T\alpha^{(l)}] - V^{(c)}[1 - T\alpha^{(c)}]\}_X} \quad (3.6)$$

where the shorthand notation $\{\dots\}_X$ specifies evaluation at point X . An equivalent description is that this expression generates a parallel family of curves parameterized by η . The $\eta=0$ member of the family of curves is the one passing precisely through point X ; this is equivalent to the function $T_H(p)$ mentioned Section 1. Eq. (3.6) thus leads to the following expression for the slope of the equal-enthalpy Kauzmann curve at X :

$$\left(\frac{dp}{dT}\right)_{\Delta H=0} = \frac{C_p^{(l)} - C_p^{(c)}}{V^{(l)}(1 - T\alpha^{(l)}) - V^{(c)}(1 - T\alpha^{(c)})} \quad (3.7)$$

Consider specifically the case $X=B$ in Fig. 1. We know that at this point of the melting curve

the liquid has a larger molar volume than the crystal. In addition, the fact that the slope of the melting curve changes from negative through zero to positive upon passing through *B* allows us to conclude from the Clausius–Clapeyron Eq. (2.1) that at $\delta p = 0$, $S^{(l)} - S^{(c)}$ and thus $H^{(l)} - H^{(c)}$ are increasing with temperature at least in linear order in δT . From Eq. (3.5) we therefore conclude that:

$$C_p^{(l)}(B) - C_p^{(c)}(B) > 0 \quad (3.8)$$

Formally, similar analyses apply to $X=D$ and to $X=E$. For both of these cases, the molar volume of the liquid is less than that of the crystal, but the sign changes of the slope of the melting curve occur in opposite directions for these latter two cases. For *D*, the slope decreases from positive, through zero, to negative as temperature increases. By contrast, the slope of the melting curve as it passes through *E* changes from negative to zero to positive with increasing temperature. These features imply that:

$$C_p^{(l)}(D) - C_p^{(c)}(D) > 0 \quad (3.9)$$

and that

$$C_p^{(l)}(E) - C_p^{(c)}(E) < 0 \quad (3.10)$$

Similar considerations can be brought to bear on the entropy functions for the two phases. Starting with the general thermodynamic relations:

$$\left(\frac{\partial S}{\partial T}\right)_p = \frac{C_p}{T} \quad (3.11)$$

and

$$\left(\frac{\partial S}{\partial p}\right)_T = -\left(\frac{\partial V}{\partial T}\right)_p = -V\alpha \quad (3.12)$$

we obtain the analog of the earlier Eq. (3.5)

$$\begin{aligned} S^{(l)}(T,p) - S^{(c)}(T,p) \cong & \left[C_p^{(l)}(X) \right. \\ & \left. - C_p^{(c)}(X) \right] \delta T / T_X \\ & - \left\{ \alpha^{(l)}(X) V^{(l)}(X) \right. \\ & \left. - \alpha^{(c)}(X) V^{(c)}(X) \right\} \delta p \end{aligned} \quad (3.13)$$

If the molar entropy difference is held fixed at some constant value, then this last relation implies that δp will have to be the following linear function of δT :

$$\begin{aligned} \delta p(\delta T, \sigma) = -\sigma + & \left\{ \frac{C_p^{(l)} - C_p^{(c)}}{T[\alpha^{(l)}V^{(l)} - \alpha^{(c)}V^{(c)}]} \right\}_X \delta T, \\ \sigma = & \frac{S^{(l)} - S^{(c)}}{(\alpha^{(l)}V^{(l)} - \alpha^{(c)}V^{(c)})_X} \end{aligned} \quad (3.14)$$

As in the case of constant enthalpy difference, this expression represents a family of parallel curves, indexed now by σ . On account of the differing denominators in Eqs. (3.14) and (3.6), the curves of fixed enthalpy difference and of fixed entropy difference will generally display distinct slopes.

The $\sigma=0$ curve from the family [Eq. (3.14)] passes through point *X*, and corresponds to vanishing entropy difference. For this special ‘Kauzmann curve’ the differential form of Eq. (3.14) then may be written:

$$\left(\frac{dp}{dT}\right)_{\Delta S=0} = \frac{C_p^{(l)} - C_p^{(c)}}{T[\alpha^{(l)}V^{(l)} - \alpha^{(c)}V^{(c)}]} \quad (3.15)$$

In principle, this same relation could be integrated to trace out an entire curve of vanishing entropy difference in the T,p plane.

It should not escape attention that Eq. (3.15) is formally identical to the first Ehrenfest relation for a line of second-order phase transitions [34]. By definition, that is a circumstance which also involves equality of molar entropies for the two phases. However, the present application is different in a fundamental way, because the curve generated by Eq. (3.15) is not a thermodynamic coexistence curve, and in particular, crossing it does not imply that an ideal glass transition has occurred.

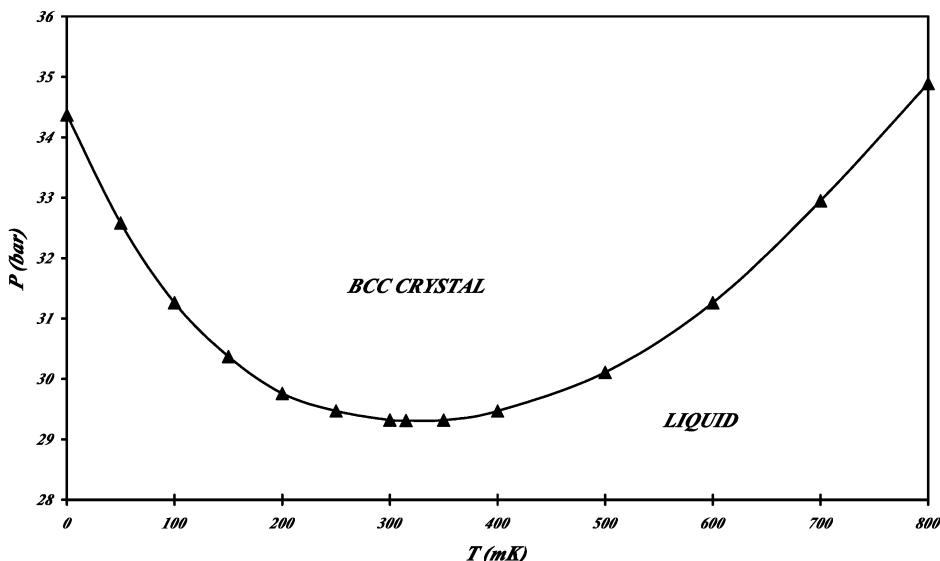


Fig. 2. Experimentally determined melting curve for ^3He , in the neighborhood of its pressure minimum. Adapted from Dobbs [23].

We close this Section 3 with a relationship obeyed by the melting curve itself, as it passes through one of the zero-slope points. When carried to second order in temperature and pressure changes, the Taylor expansion of chemical potential is:

$$\begin{aligned} \mu(\delta T, \delta p) = & \mu(X) - S(X)\delta T + V(X)\delta p \\ & - \left(\frac{C_p(X)}{2T_X} \right) (\delta T)^2 + V(X)\alpha(X)\delta T\delta p \\ & - \left(\frac{V(X)\kappa_T(X)}{2} \right) (\delta p)^2 + \dots \end{aligned} \quad (3.16)$$

Along the melting curve, the chemical potentials of the two phases must be equal. Furthermore, in the immediate vicinity of the zero-slope points such as *B*, *D* and *E*, the pressure δp along the melting curve is proportional to $(\delta T)^2$. By utilizing these properties in connection with the Taylor expansion [Eq. (3.16)], one obtains the following expression for the second temperature derivative of the melting curve at zero-slope points:

$$\frac{d^2 p_m}{dT^2} = \frac{C_p^{(l)} - C_p^{(c)}}{T(V^{(l)} - V^{(c)})} \quad (3.17)$$

This indicates that points *B* and *E*, exhibiting upward curvature in Fig. 1, must have a common sign for the heat capacity difference, and the volume difference, between the phases. By contrast, point *D* must entail opposite signs for these quantities.

Distinct positive or negative signs in principle can occur for the various combinations of thermodynamic quantities that appear as factors in the basic enthalpy and entropy Eqs. (3.7) and (3.15). Those signs jointly determine the signs of the slopes of the enthalpy and entropy Kauzmann curves as they pass through the zero-slope points of the melting curve. The slopes of those curves in principle can be either positive or negative, and need not be the same for the vanishing-enthalpy and vanishing-entropy loci at any given zero-slope point of the melting curve.

4. Melting curve for ^3He

We now examine in quantitative detail the inverse melting phenomenon for ^3He . As mentioned earlier, a melting-curve minimum of type *B* in Fig. 1 is involved. This example has had a notable technical application, specifically in the ‘Pomeranchuk refrigerator’ that attains millikelvin

Table 1

Experimentally measured values of thermodynamic properties for the coexisting liquid and crystal phases of ^3He , at the zero-slope melting minimum^a

Property	Measured value
T (K)	0.315
p (bar)	29.31
d^2p_m/dT^2 (bar K ⁻²)	70
$V^{(c)}$ (cm ³ mol ⁻¹)	24.80
$V^{(l)}$ (cm ³ mol ⁻¹)	26.04
$\alpha^{(c)}$ (K ⁻¹)	0.00070
$\alpha^{(l)}$ (K ⁻¹)	-0.00696

^a All entries have been extracted from data presented in the extensive review by Dobbs [23].

temperatures in the laboratory [35]. Fig. 2 shows that part of the melting curve for this substance that is relevant to our inverse melting discussion, specifically the vicinity of the zero-slope pressure minimum. Measured values of various thermodynamic properties at that minimum have been collected in Table 1.

In contrast to the other inverse-melting examples mentioned in Section 2 above, the helium isotopes are distinctly quantum mechanical in their behavior. This is particularly so with the fermionic lighter isotope ^3He , for which the deep melting curve minimum owes its existence to the involvement of nuclear spin degrees of freedom. These nuclear spins are relatively free to reorient independently in the crystal at the temperature range of concern here, thereby increasing entropy. By contrast, particle exchange in the ^3He liquid strongly couples nuclear spins in that phase, so the entropy remains low in comparison to the crystal. The bosonic heavier isotope ^4He has no nuclear spin, and its very shallow melting curve minimum relies on the relative phonon densities of states for the crystal and liquid phases [8].

By inserting values from Table 1 into the p_m curvature condition Eq. (3.17), one can evaluate the heat capacity difference at the melting-point minimum:

$$C_p^{(l)} - C_p^{(c)} \cong 2.73 \text{ J mol}^{-1} \text{ K}^{-1} \quad (4.1)$$

which is consistent with the inequality of Eq.

(3.8). This leads in turn, to numerical evaluation of the slope of the equal-entropy Kauzmann curve, Eq. (3.15), as it passes through the melting point minimum:

$$\left(\frac{dp}{dT}\right)_{\Delta S=0} \cong -437 \text{ bar K}^{-1} \quad (4.2)$$

In a similar fashion, the slope of the equal-enthalpy curve at the same point can be evaluated from Eq. (3.7):

$$\left(\frac{dp}{dT}\right)_{\Delta H=0} \cong -21.0 \text{ bar K}^{-1} \quad (4.3)$$

5. Discussion

The point E included in the schematic Fig. 1 involves liquid at higher pressure than the crystal, and positive curvature to the melting curve at this zero-slope point. Currently, no known real-world example exists for this combination of attributes, but nothing in principle seems to exclude it. Although not included in Fig. 1 in the interest of simplicity, a phase-reversed version of point D can also be imagined, displaying liquid at lower pressure than crystal, and (as with D itself) negative second derivative for the melting curve at that zero-slope point. Again, no known real-world example with this characteristic currently exists.

All cases of inverse melting appear to involve, and probably require, a significant number of microscopic degrees of freedom that are coupled to the particle center-of-mass degrees of freedom. It is localization of the latter that determine freezing of a liquid into a spatially periodic solid. Nuclear spins play this role of coupled degrees of freedom in ^3He . Backbone and side-group conformational degrees of freedom evidently play an analogous part for the polymeric substance P4MP1. The ribonuclease A and liquid–crystal cases cited in Section 2 above also possess many internal molecular degrees of freedom that are coupled respectively to native-state conformation, and to orientational and positional order to produce inverse melting analogs. One might say that a

preponderance of internal degrees of freedom, when properly coupled to molecular position, have the capacity to drive inverse melting phenomena.

These last considerations offer hope for the construction of theoretical many-body models that upon analytical and/or simulational examination will exhibit inverse melting. Within the regime of classical statistical mechanics, one such opportunity may emerge from a suitably crafted polymer model. It was pointed out by Flory and Krigbaum many years ago [36] that polymers suspended in suitable solvents experience repulsive effective pair interactions that are essentially Gaussian functions of the centroid-to-centroid distance. This observation can be abstracted into the well-studied Gaussian core model [37–39], which is known to have a point of type *C*, Fig. 1, at which the melting volume changes sign. At present, a study is underway to insert ‘polymer’ internal degrees of freedom into the Gaussian core model that implicitly change its centroid-to-centroid effective interactions as temperature changes. In fact, it has been established that under proper circumstances, an inverse melting phenomenon can arise [40].

Finally, we return to remark about the Kauzmann curves, specifically those for entropy equality of liquid and crystal phases. The results deduced in this paper add a new facet to the interpretation of the glass transition, and to the related ‘Kauzmann paradox’. We have shown that at least for those few systems which exhibit inverse melting, a Kauzmann curve of equal entropies is not itself a line of phase transitions in the T,p plane. It is conceivable that some inverse melting systems might also have glass transitions, and that continuation of the equal-entropy curve from the locale upon which we have focused to that glass transition locale might encounter the conventional Kauzmann temperature. We therefore raise the question whether the Kauzmann temperature for supercooled liquids necessarily implies the existence of an ideal glass transition (never directly observed, of course). It appears to be an equally plausible proposition that Kauzmann curves for supercooled liquids are simply an interesting thermodynamic locus, without demanding an interpretation as an ideal glass transition.

Acknowledgments

PGD gratefully acknowledges financial support by the US Department of Energy, Division of Chemical Sciences, Geosciences, and Biosciences, Office of Basic Energy Sciences (Grant DE-FG02-87ER13714).

References

- [1] W. Kauzmann, The nature of the glassy state and the behavior of liquids at low temperatures, *Chem. Rev.* 43 (1948) 219–256.
- [2] J. Jäckle, Models of the glass transition, *Rep. Prog. Phys.* 49 (1986) 171–231.
- [3] M.D. Ediger, C.A. Angell, S.R. Nagel, Supercooled liquids and glasses, *J. Phys. Chem.* 100 (1996) 13200–13212.
- [4] P.G. Debenedetti, *Metastable Liquids: Concepts and Principles*, Princeton University Press, Princeton, NJ, 1996.
- [5] C.A. Angell, K.L. Ngai, G.B. McKenna, P.F. McMillan, S.W. Martin, Relaxation in glassforming liquids, *J. Appl. Phys.* 88 (2000) 3113–3157.
- [6] P.G. Debenedetti, F.H. Stillinger, Supercooled liquids and the glass transition, *Nature* 410 (2001) 259–267.
- [7] H.B. Callen, *Thermodynamics*, John Wiley and Sons, New York, 1985, p. 30.
- [8] F.H. Stillinger, P.G. Debenedetti, T.M. Truskett, The Kauzmann paradox revisited, *J. Phys. Chem. B* 105 (2001) 11809–11816.
- [9] H. Vogel, Das temperature-abhängigkeitsgesetz der viskosität von flüssigkeiten, *Phys. Zeit.* 22 (1921) 645–646.
- [10] G. Tammann, W. Hesse, Die abhängigkeit der viskosität von der temperature bei unterkühlten flüssigkeiten, *Z. Anorg. Allg. Chem.* 156 (1926) 245–257.
- [11] G.S. Fulcher, Analysis of recent measurements of the viscosity of glasses, *J. Am. Ceram. Soc.* 8 (1925) 339–355.
- [12] G. Adam, J.H. Gibbs, On the temperature dependence of cooperative relaxation properties in glass-forming liquids, *J. Chem. Phys.* 43 (1965) 139–146.
- [13] P.G. Debenedetti, F.H. Stillinger, T.M. Truskett, C.J. Roberts, The equation of state of an energy landscape, *J. Phys. Chem. B* 103 (1999) 7390–7397.
- [14] M. Utz, P.G. Debenedetti, F.H. Stillinger, Isotropic tensile strength of molecular glasses, *J. Chem. Phys.* 114 (2001) 10049–10057.
- [15] J. Jäckle, Models of the glass transition, *Rep. Prog. Phys.* 49 (1986) 171–231.
- [16] F.H. Stillinger, Supercooled liquids, glass transitions, and the Kauzmann paradox, *J. Chem. Phys.* 88 (1988) 7818–7825.

- [17] P.G. Debenedetti, F.H. Stillinger, C.P. Lewis, Model energy landscapes, unpublished manuscript.
- [18] W. Kauzmann, Some factors in the interpretation of protein denaturation, *Adv. Protein Chem.* 14 (1959) 1–63.
- [19] H. Reiss, *Methods of Thermodynamics*, Dover, Mineola, NY, 1996, p. 137.
- [20] D.A. Young, *Phase Diagrams of the Elements*, University of California Press, Berkeley, 1991.
- [21] D. Eisenberg, W. Kauzmann, *The Structure and Properties of Water*, Oxford University Press, New York, 1969.
- [22] G. Tammann, *Kristallisieren und Schmelzen*, Johann Ambrosius Barth, Leipzig, 1903, pp. 26–46.
- [23] E.R. Dobbs, *Helium Three*, Oxford University Press, Oxford, 2002.
- [24] C. Le Pair, K.W. Taconis, R. De Bruyn Ouboter, P. Das, A direct measurement of the minimum in the melting curve of ^4He , *Physica* 29 (1963) 755–756.
- [25] J. Wilks, *The Properties of Liquid and Solid Helium*, Clarendon Press, Oxford, 1967.
- [26] S. Rastogi, M. Newman, A. Keller, Pressure-induced amorphization and disordering on cooling in a crystalline polymer, *Nature* 353 (1991) 55–57.
- [27] S. Rastogi, M. Newman, A. Keller, Unusual pressure-induced phase behavior in crystalline poly-4-methylpentene-1, *J. Polym. Sci. (Polym. Phys.) B* 31 (1993) 125–139.
- [28] S. Rastogi, G.W.H. Höhne, A. Keller, Unusual pressure-induced phase behavior in crystalline poly(4-methylpentene-10): calorimetric and spectroscopic results and further implications, *Macromolecules* 32 (1999) 8897–8909.
- [29] A.L. Greer, Too hot to melt, *Nature* 404 (2000) 134–135.
- [30] J. Zhang, X. Peng, A. Jonas, J. Jonas, NMR study of the cold, heat, and pressure unfolding of ribonuclease A, *Biochemistry* 34 (1995) 8631–8641.
- [31] P.E. Cladis, D. Guillon, F.R. Bouchet, P.L. Finn, Reentrant nematic transitions in cyano-octyloxybiphenyl (8OCB), *Phys. Rev. A* 23 (1981) 2594–2601.
- [32] G.P. Johari, The Tammann phase boundary, exothermic disordering and the entropy contribution change on phase transformation, *Phys. Chem. Chem. Phys.* 3 (2001) 2483–2487.
- [33] W. Sinkler, C. Michaelson, R. Bormann, A transmission electron microscopy investigation of inverse melting in $\text{Nb}_{45}\text{Cr}_{55}$, *J. Mater. Res.* 12 (1997) 1872–1884.
- [34] A.B. Pippard, *The Elements of Classical Thermodynamics*, Cambridge University Press, Cambridge, 1957, p. 140.
- [35] J. Wilks, D.S. Betts, *An Introduction to Liquid Helium*, Clarendon Press, Oxford, 1987, pp. 79–80.
- [36] P.J. Flory, *Principles of Polymer Chemistry*, Cornell University Press, Ithaca, 1953, p. 539.
- [37] F.H. Stillinger, D.K. Stillinger, Negative thermal expansion in the Gaussian core model, *Physica A* 244 (1997) 358–369.
- [38] A. Lang, C.N. Likos, M. Watzlawek, H. Löwen, Fluid and solid phases of the Gaussian core model, *J. Phys. Condens. Matter* 12 (2000) 5087–5108.
- [39] A.A. Louis, P.G. Bolhuis, J.P. Hansen, Mean field fluid behavior of the Gaussian core model, *Phys. Rev. E* 62 (2000) 7961–7972.
- [40] M.R. Feeney, P.G. Debenedetti, F.H. Stillinger, *J. Chem. Phys.*, submitted.